Sub-Network Kernels for Measuring Similarity of Brain Connectivity Networks in Disease Diagnosis

Biao Jie⬛, Mingxia Liu, Daoqiang Zhang, and Dinggang Shen, *Fellow, IEEE*

Abstract—As a simple representation of interactions among distributed brain regions, brain networks have been widely applied to automated diagnosis of brain diseases, such as Alzheimer's disease (AD) and its early stage, *i.e.*, mild cognitive impairment (MCI). In brain network analysis, a challenging task is how to measure the similarity between a pair of networks. Although many graph kernels (*i.e.*, kernels defined on graphs) have been proposed for measuring the topological similarity of a pair of brain networks, most of them are defined using general graphs, thus ignoring the uniqueness of each node in brain networks. That is, each node in a brain network denotes a particular brain region, which is a specific characteristics of brain networks. Accordingly, in this paper, we construct a novel sub-network kernel for measuring the similarity between a pair of brain networks and then apply it to brain disease classification. Different from current graph kernels, our proposed sub-network kernel *not only* takes into account the inherent characteristic of brain networks, *but also* captures multi-level (from local to global) topological properties of nodes in brain networks, which are essential for defining the similarity measure of brain networks. To validate the efficacy of our method, we perform extensive experiments on subjects with baseline functional magnetic resonance imaging data obtained from the Alzheimer's disease neuroimaging initiative database. Experimental results demonstrate that the proposed method outperforms several state-of-the-art graph-based methods in MCI classification.

Index Terms—Graph kernel, brain network, Alzheimer's disease (AD), mild cognitive impairment (MCI), classification.

I. INTRODUCTION

AS A NEURODEGENERATIVE disorder, Alzheimer's disease (AD) is the most common form of dementia in elderly population worldwide, which usually starts slowly and gets worse over time. In general, AD leads to substantial, progressive neuron damage that is irreversible, which eventually causes death. Recently, a prodromal stage of AD called mild cognitive impairment (MCI) has gained increasing attention, due to its high probability of progression to AD. It is reported the patients with MCI will progress to clinical AD at an annual rate of approximately 10% to 15%, while normal controls (NCs) will develop dementia at an annual rate of 1% to 2% [1]. In addition, disease-modifying therapies, given to patients at the early stage of their disease development, will have better effect in slowing down the disease progression and helping preserve some cognitive functions of the brain. Thus, accurate diagnosis of MCI is very important for early treatment and possible delay of AD progression.

A large amount of evidences from both anatomical and physiological studies suggest that cognitive processes depend on interactions among distributed brain regions [2]. In the past years, some new emerging medical imaging techniques, such as modern magnetic resonance imaging (MRI) and functional MRI (fMRI), have provided non-invasive ways to map the patterns of structural and functional interaction of brain regions [3], [4]. These interaction patterns can be characterized as brain networks, thus helping us better understand the pathological underpinnings of neurological disorder by exploring connectivity in brain networks. For example, fMRI provides an opportunity to quantify functional interaction by measuring the correlation between intrinsic blood oxygen level-dependent (BOLD) signal fluctuations of distributed brain regions at rest. Accordingly, functional connectivity networks have been widely used in brain disease analysis [5]–[7].

Among various studies for brain network analysis, graph theory provides an effective solution to concisely quantify the connectivity properties of networks, where each node denotes a particular anatomical element (*e.g.*, a brain region) and each edge represents the relationship (*e.g.*, connectivity) between a pair of nodes. However, different from traditional data that can be represented in a feature space, data in the form of graph

B. Jie is with the Department of Radiology and BRIC, University of North Carolina at Chapel Hill, NC 27599 USA, also with the Department of Computer Science and Technology, Anhui Normal University, Wuhu 241003, China, and also with the Anhui Provincial Key Laboratory of Network and Information Security, Wuhu 241003, China.

M. Liu is with the Department of Radiology and BRIC, University of North Carolina at Chapel Hill, NC 27599 USA.

D. Zhang is with the Department of Computer Science and Engineering, Nanjing University of Aeronautics and Astronautics, Nanjing 210016, China (e-mail: dqzhang@nuaa.edu.cn).

D. Shen is with the Department of Radiology and BRIC, University of North Carolina at Chapel Hill, NC 27599 USA, and also with the Department of Brain and Cognitive Engineering, Korea University, Seoul 02841, South Korea (e-mail: dgshen@med.unc.edu).

This paper has supplementary downloadable material available at http://ieeexplore.ieee.org, provided by the author. The material includes tables of data relevant to the main paper. The total size of the file is 0.0811 MB. Contact dgshen@med.unc.edu for further questions about this work.

Color versions of one or more of the figures in this paper are available online at http://ieeexplore.ieee.org.

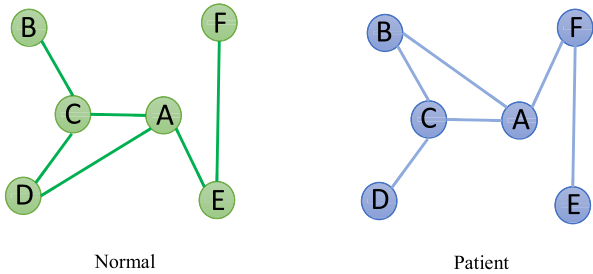Digital Object Identifier 10.1109/TIP.2018.2799706

Fig. 1. Examples of brain networks illustrating a normal control (left) and a MCI patient (right). Note that some connections in the patient's network have been changed. These two brain networks are isomorphic when ignoring the label information of each node; thus, the similarity between these two networks without using label information will be not their actual similarity.
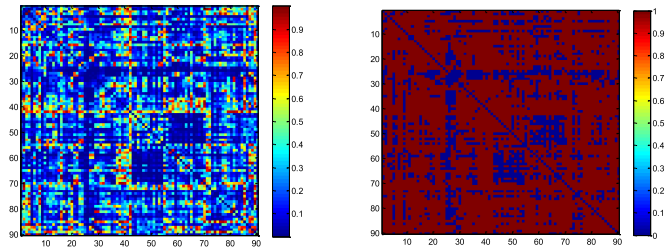

Fig. 2. The discriminative power of each connection in brain networks in identification 99 MCI patients and 50 normal controls using the standard *t*-test on a ADNI database. (Left) The *p*-values on connections between all pairs of brain regions (or graph nodes). (Right) The corresponding thresholded *p*-values (*i.e.*, by setting *p*-values more than 0.05 to 1).

cannot be directly represented by feature vectors. Hence, it is challenging to determine how to compare (*i.e.*, measure the similarity of) a pair of graphs, which is a fundamental problem in graph-based analysis. To deal with this problem, many studies have been focused on defining the similarity among graphs (*i.e.*, networks) in the last decade.

Among various methods for computing the graph similarity, kernel methods [8] offer a natural framework to study this problem. In particular, graph kernels, *i.e.*, the kernels constructed on graphs, have been proposed and applied to brain network analysis. However, most of the existing graph kernels ignore the uniqueness of each node in brain networks, which is an inherent characteristics of brain networks. That is, after registering brain images of all subjects into a common space, each node in the brain networks is uniquely corresponding to a specific brain region (denoted by a letter or number, called as label of the node). Previous graph kernels seldom take advantage of the uniqueness of each node, due to the difficulty of computing the similarity between brain networks. Fig. 1 illustrates an example of brain networks for a NC and an MCI patient, where each node corresponds to a specific brain region (denoted by a letter). Since the connections in the patient's brain network have been affected by the disease, these two brain networks in Fig. 1 are isomorphic if ignoring the label information of each node. Obviously, based on the existing graph kernels without using the label information, the similarity of two networks can not reflect the real topological characteristics of these networks.

Numerous studies have suggested that neurodegenerative diseases (*e.g.*, AD and MCI) are related to connectivity among specific brain regions [6], [9], [10]. Therefore, both local and global topological properties on brain regions are very important for brain network analysis. Figure 2 illustrates the discriminative power of each connection in brain networks between 99 MCI patients and 50 normal controls using the standard *t*-test on a real dataset from Alzheimer's disease Neuroimaging Initiative (ADNI).[1] The characteristics of these subjects and the corresponding brain networks are presented in Sections III-A and III-B, respectively. Here, Fig. 2 (a) shows the obtained *p*-values on all connections, and Fig. 2 (b) shows the thresholded *p*-values (*i.e.*, by setting *p*-values more than

0.05 to 1). From Fig. 2 (a)-(b), it can be seen that lots of discriminative connections (with their corresponding *p*-values less than 0.05) mainly distribute on several specific brain regions. Intuitively, exploring both local and global connectivity properties of brain regions can construct more effective kernels for measuring the similarity of brain networks. To the best of our knowledge, we are among the first to exploit both local and global connectivity properties of brain regions to construct graph kernels for measuring the similarity of brain networks.

Motivated by a recent work in [11], in this paper, we propose a novel sub-network kernel on brain networks for brain disease classification. Specifically, we first construct a group of sub-networks on each node to reflect the multi-level (*i.e.*, from local to global) connectivity properties of brain networks. Then, we define the similarity of a pair of brain networks, by calculating the similarities of all corresponding pairs of sub-network groups when considering the uniqueness of nodes. Different from traditional graph kernels, our sub-network kernel not only takes into account the inherent characteristics of brain network, but also captures the multi-level topological properties on nodes of brain networks. We evaluate our proposed method on 183 subjects with the baseline resting-state fMRI (rs-fMRI) data from the ADNI database, which contains 50 normal controls, 99 MCI patients and 34 AD patients. The experimental results demonstrate the efficacy of our proposed method.

The main contributions of this paper are three-fold. *First*, we define a novel sub-network kernel for measuring the similarity between brain networks. To the best of our knowledge, our proposed method is among the first attempts to build brain-network-oriented kernel by utilizing the specific characteristics of brain network. *Second*, we develop a sub-network kernel based learning (SKL) framework for automated brain disease diagnosis based on fMRI data. *Finally*, we provide an implementation for performing inference on brain network data.

The rest of the paper is organized as follows. In Section II, we briefly review the related studies. Then, we describe the data used in current study, and present the proposed method and classification framework in Section III. In Section IV, we introduce experimental setting and results. In Section V, we give discussions for the experimental results, the influence of parameters, and the limitation of our method. Finally, we conclude this paper in Section VI.

[1] http://adni.loni.usc.edu/

II. RELATED WORKS

A. Graph-Based Methods

Graph theory has been successfully applied to investigate brain networks related to various diseases [12], [13]. For example, studies have investigated the local connectivity properties of brain networks for AD/MCI patients by using graph-theory-based approaches, and reported a series of abnormal structural and functional connectivity, including the disrupted functional connectivity between the hippocampus and other brain regions [14], [15], and also the decreased functional connectivity with a network of posterior cingulate cortex, temporoparietal junction, and hippocampus [16]. Also, other studies have investigated the global topological characteristics of functional brain networks, and found that the small-world characteristics (*i.e.*, high degree of clustering and short path length) have been disrupted in AD patients [9]. Besides, a similar study has also investigated the topological organization of brain networks in the apolipoprotein E epsilon 4 allele (APOE-4) carriers, where APOE-4 is a major genetic determinant for AD [17]. More recently, graph theory has been applied to automatic diagnosis of brain diseases, *e.g.*, AD and MCI [18]–[21].

Compared with other brain network analysis approaches, graph theory offers two important advantages [6]. First, it provides quantitative measurement of each node, which can preserve the connectivity information in the network and thus reflect the segregated and integrated nature of local brain activity. For example, the clustering coefficient [22], which quantifies the degree to which nodes in a graph tend to cluster together, is one of the simplest and most common measures of functional segregation in brain network analysis. Researchers have investigated the local clustering properties of functional connectivity networks, and found the disruption of local clustering in AD/MCI patients [14], [15]. This may indicate that the functional connectivity network becomes less modular and thus the efficient organization for information transferring is lost for AD/MCI patients [15], [19], [23].

Another advantage of graph theory is that it provides a general framework for comparing heterogeneous graphs constructed using different types of data (*e.g.*, anatomical and functional data). Therefore, graph theory shows great promise to disentangle how various pathological processes in brain diseases develop, and provides a possible way to identify image-based biomarkers for automated diagnosis of brain diseases [6], [7], [24]. For example, the clustering coefficients from structural and functional connectivity networks have been used for the classification of MCI individuals [7], [25].

B. Network Similarity Measurement

Among various network similarity measurement methods, one simple and straightforward approach is to extract some local measures of networks (*e.g.*, edge weights, path lengths, and clustering coefficients) as feature vectors for computing network similarity and performing network analysis. For example, Chen *et al.* [26] used connectivity strengths between the brain region pairs as features for AD/MCI classification. Wee *et al.* [27] extracted clustering coefficients from white matter connectivity networks as features for identification of MCI patients. Zanin *et al.* [28] explored sixteen topological features from functional connectivity networks to find the optimal network representation. Also, Tijms *et al.* [6] investigated 13 graph properties and examined which properties have been consistently reported to be disturbed in AD studies by using group analysis. These studies demonstrate the advantages of graph theory in neuroimaging data analysis. However, these methods usually composite the local topological measures of brain networks as feature vectors, and thus lose their global topology characteristics.

In addition, kernel methods offer a natural framework to study the similarity of networks. Informally, a kernel is a function that measures the similarity between a pair of objects, which mathematically corresponds to an inner product in a reproducing kernel Hilbert space [8], [29]. Once a kernel is defined, many learning algorithms such as support vector machines (SVM) can be applied directly, which facilitates the subsequent classification/regression tasks. In the literature, graph kernels, *i.e.*, the kernels constructed on graphs, have been proposed and applied to diverse fields including neuroimaging studies [30]–[32], image classification [33], and protein function prediction [34]. Kernel methods have been recently applied to brain network classification, such as classification of patients with brain disease and normal controls [35]–[37] as well as classification of task-related state and resting state [30].

Graph kernels are instances of the family of so-called R-convolution kernels by Haussler [38]. Most of graph kernels are defined via comparing small sub-graphs such as walks [39], paths, or graphlets [40]. Since searching for structural similarities in a pair of graphs is often computationally expensive, some researchers explore graph kernels with lower computational complexity by using computational techniques [41]. Recently, researchers have defined an effective graph kernel via building a new mathematical representation for graphs [11]. Other researchers have also constructed graph kernels by using geometric embedding approach [42]. Compared with feature-based methods, kernel-based methods can capture both local and global topological properties of graphs, and thus usually achieve better performance in brain network classification. In general, the existing graph kernels can be roughly divided into two categories: 1) *kernels defined on unlabeled graphs* where each node has no distinct identification except using their interconnectivity, such as graph kernels in [11], [40], and [42]; 2) *kernels defined on labeled graphs* where each node is labeled with different letter, such as graph kernels used in [41] and [39]. Note that some graph kernels, *e.g.*, those used in [43], can be defined on both labeled graphs and unlabeled graphs.

In the first category, graph kernels defined on the unlabeled graphs can also be used for computing the similarity of labeled graphs by ignoring their label information, but this may make those graph kernels not able to compute the actual similarity of labeled graphs. See Fig. 1 for example, where graph kernels defined on unlabeled graphs will fail to measure the actual similarity of two brain networks in Fig. 1. Besides, most graph kernels in the second category are not suitable to compare
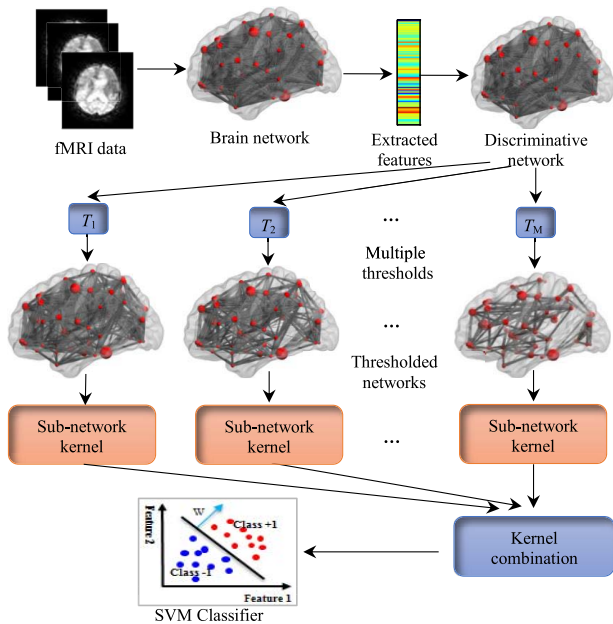
Fig. 3. Illustration of the sub-network kernels based learning (SKL) framework.

the similarity of a pair of brain networks, because some graph kernels are infeasible for brain networks due to their computational complexity [39], [44]. Also, some graph kernels in this category cannot be computed on the brain networks. For instance, graph kernels in [44] are used to compare graphs with edge labels, and graph kernels in [41] are used to compare graphs with continuous-valued node labels. Other graph kernels such as those in [43] are constructed based on the Weisfeiler-Lehman test of graph isomorphism. However, no graph isomorphism problem exists, when considering the specific information of each node on brain networks.

To address these problems, in this paper we propose a novel sub-network kernel for measuring similarity of brain networks.

III. MATERIALS AND METHOD

Figure 3 illustrates our proposed sub-network kernel based learning (SKL) framework for brain disease classification, which includes three main steps: (1) image preprocessing and connectivity network construction, (2) network thresholding and sub-network kernel construction, and (3) classification. In this section, we first introduce the data used in this study, and then present the details of each step in our proposed framework.

A. Subjects

In this study, we use a total of 183 subjects, which includes 50 normal controls, 99 MCI patients and 34 AD patients, each with fMRI. Among 99 MCI subjects, there are 56 early MCI (EMCI) and 43 late MCI (LMCI) subjects. Table S1 in the *Supporting Information* gives the ID of those subjects. All rs-fMRI data were acquired on 3.0 Tesla Philips scanners (with varied models/systems) at multiple sites. There is a range for imaging resolution in *X* and *Y* dimensions,

TABLE I
CHARACTERISTICS OF THE SUBJECTS (MMSE ± STANDARD DEVIATION). MMSE: MINI-MENTAL STATE EXAMINATION

Group	NC	MCI	AD
Male/Female	21/29	47/52	18/16
Age (Mean ± SD)	75.0 ± 6.9	71.7 ± 7.4	72.8 ± 7.2
MMSE (Mean ± SD)	28.9 ± 1.6	27.8 ± 1.8	21.4 ± 3.1

which is from 2.29 mm to 3.31mm and the slice thickness is 3.31mm. TE (echo time) for all subjects is 30ms and TR (repetition time) is from 2.2s to 3.1s. For each subject, there are 140 volumes (time points). All rs-fMRI data can be downloaded from the ADNI database. Table I reports the demographic and clinical information of the studied subjects.

B. Image Preprocessing and Network Construction

We perform image pre-processing for all rs-fMRI data using a standard pipeline, including brain skull removal, slice time correction, motion correction, spatial smoothing, and temporal pre-whitening using FSL FEAT software package (http://fsl.fmrib.ox.ac.uk/fsl/fslwiki/FEAT). Specifically, the acquired rs-fMRI images are corrected for the acquisition time difference among all slices. All images are then aligned to the first volume for motion correction and a brain mask is also created from the first volume. At last, the global drift removal and band pass filtering between 0.01Hz–0.1Hz are performed using tool in [45]. The pre-processing steps of the T1-weighted data include brain skull removal and tissue segmentation into gray matter (GM), white matter (WM), and cerebrospinal fluid (CSF) using FSL FAST software package (http://fsl.fmrib.ox.ac.uk/fsl/fslwiki/FAST). The pre-processed T1 image is then co-registered to the first volume of the pre-processed rs-fMRI data of the same subject and the BOLD signals in GM are merely extracted and adopted to avoid the relatively high proportion of noise caused by the cardiac and respiratory cycles in WM and ventricle [46]. Finally, the whole brain of each subject in rs-fMRI space is parcellated into 90 regions of interest (ROI), by warping the automated anatomical labeling (AAL) template [47] to the rs-fMRI image space of each subject using the FSL FLIRT software package (http://fsl.fmrib.ox.ac.uk/fsl/fslwiki/FLIRT). For each of the 90 ROIs, the mean rs-fMRI time series was calculated by averaging the GM-masked BOLD signals among all voxels within the specific ROI. Finally, we use *Pearson correlation coefficients* to build functional connectivity between the ROIs. Specifically, for each subject, we construct a fully-connected functional connectivity network, where each node corresponds to a particular ROI and the edge weight is the Pearson correlation coefficient of a pair of specific ROIs. Then, we apply Fisher's r-to-z transformation on the elements of the functional connectivity network to improve the normality of the correlation coefficients.

C. Proposed Sub-Network Kernel

In this section, we first introduce some related notations. Then, we briefly introduce the existing studies in [11].

Motivated by that work, we propose our graph kernels. In the rest of the paper, we use P_{ij} to denote the entry (i, j) of matrix P.

Defintion 1 (Graph): A graph $\mathcal{G}$ can be defined as a pair, *i.e.*, $\mathcal{G} = (V, E)$, where V is a set of nodes, and E is a set of edges between nodes, *i.e.*, $E \subseteq \{(u, v)|u, v \in V\}$.

Defintion 2 (Sub-Graph): A graph $\mathcal{G}' = (V', E')$ is a subgraph of another graph $\mathcal{G} = (V, E)$ iff $V' \subseteq V$ and $E' \subseteq \{(u, v)|(u, v) \in E \wedge u, v \in V'\}$

According these definitions, the graph and sub-graph are binary graph, there is no weight information on edges in graph or sub-graph. We denote $W \in R^{N \times N}$ as the adjacency matrix for a graph $\mathcal{G}$, where $W_{ij} = 1$ if there has an edge between nodes i and j; otherwise, $W_{ij} = 0$. And, N is the number of nodes in $\mathcal{G}$. To effectively represent a graph, Shrivastava and Li [11] defined a symmetric positive semidefinite covariance matrix $C \in R^{d \times d}$ with

$$C_{ij} = cov(\frac{N W^i e}{\|W^i e\|_1}, \frac{N W^j e}{\|W^j e\|_1}) \qquad (1)$$

where cov denotes the covariance between two vectors, $W^i e$ denotes the i-th power iteration of matrix W on a given starting vector e (*i.e.*, the vector of all ones), and d represents the number of power iterations, which also controls the number of algorithm iterations in this new mathematical representation for the graph $\mathcal{G}$. Also, the term $\|\cdot\|_1$ denotes the l_1 norm of a vector. Here, the set of power iterations on a given vector v, *i.e.*, $\{v, Wv, W^2v, \cdots, W^d v\}$, is known as the "$d$-order Krylov subspace", which contains sufficient information to describe the associated matrix W for some appropriately chosen d. Let $v = e$ which makes the covariance between different pairs of vectors in the power iteration being "graph invariant" (*i.e.*, with the same representation for isomorphic graphs).

Shrivastava and Li [11] have argued that the matrix C can capture critical information of the underlying graph, including the spectrum of adjacency matrix W as well as counts of various sub-structures (*e.g.*, the number of triangles and the number of small paths, *etc.*), and owns many good properties, such as graph invariant. According to the definition in Eq. 1, different kinds of graphs or sub-graphs can be represented in a common mathematical space and thus directly compared to each other.

Motivated by this work, we propose a novel sub-network (*i.e.*, sub-graph) kernel for measuring similarity between a pair of brain networks. Specifically, we first construct a group of sub-networks on each node to reflect the multi-level (*i.e.*, from local to global) connectivity properties of a brain network. Then, we can compute the similarity of brain networks by calculating the similarities of all pairs of sub-network groups from the same node across different brain networks, since each node in a brain network is corresponding to a particular brain region and is thus unique.

Specifically, we denote $\mathcal{G} = (V, E)$ and $\mathcal{H} = (V, E')$ as a pair of brain networks (*i.e.*, corresponding thresholded functional-connectivity-networks in current studies, as shown in Fig. 3), where V denotes the corresponding node set for both brain networks since they share the same nodes
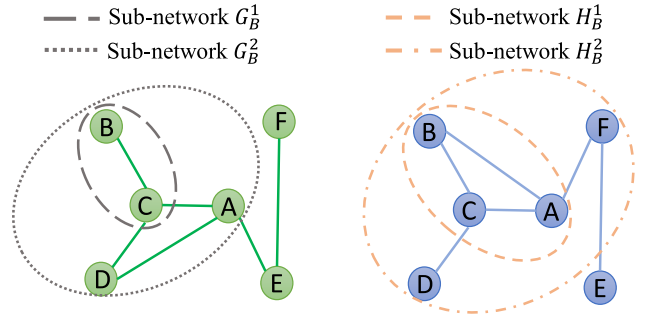

Fig. 4. Illustration of process of constructing two sub-network sets at the node B on a pair of brain networks $\mathcal{G}$ (left) and $\mathcal{H}$ (right) with $h = 2$. Here, $\{G_B^j\}_{j=1,2}$ and $\{H_B^j\}_{j=1,2}$ are two sub-network sets constructed on node B, where G_B^j and H_B^j are two sub-networks that consist of node B and nodes with their shortest-path length to B less than or equal to j.

(*w.r.t.* brain regions). Also, E and E' denote the corresponding edge sets for $\mathcal{G}$ and $\mathcal{H}$, respectively. To reflect the multi-level topological properties of brain networks, we first define two sets of sub-networks on each node v_i in the networks $\mathcal{G}$ and $\mathcal{H}$, *i.e.*,

$$\mathcal{G}_i^h = \{G_i^j = (V_i^j, E_i^j)\}_{j=1,2,\cdots,h}$$
$$\mathcal{H}_i^h = \{H_i^j = (V'_i^j, E'_i^j)\}_{j=1,2,\cdots,h} \qquad (2)$$

where $V_i^j = \{v \in V|s(v, v_i) \leq j\}$, $E_i^j = \{(u, v) \in E|u, v \in V_i^j\}$, $V'_i^j = \{v \in V|s(v, v_i) \leq j\}$, $E'_i^j = \{(u, v) \in E'|u, v \in V'_i^j\}$, and $s(\cdot, v_i)$ denotes the length of the shortest-path between node v_i and other. Here, h determines the maximum of $s(\cdot, v_i)$ (*i.e.*, $s(\cdot, v_i) \leq h$), and also defines the number of sub-networks in the set $\mathcal{G}_i^h$ and the set $\mathcal{H}_i^h$.

According to Eq. (2), G_i^j denotes a sub-network defined on the node v_i from the original networks $\mathcal{G}$, where V_i^j represents the corresponding node set which consists of node v_i and the nodes with their shortest path length to node v_i less than or equal to j, and E_i^j represents the corresponding set of edges occurred in $\mathcal{G}$. So, G_i^j reflects the topological properties of node v_i. And, G_i^j with larger value of j usually contain more nodes and edges, thus reflecting more global topological properties of node v_i. Therefore, the sub-network set $\mathcal{G}_i^h = \{G_i^j\}_{j=1,2,\cdots,h}$ reflects the multi-level (*i.e.*, from local to global) topological properties of node v_i. Fig. 4 illustrates an example of the construction process for two groups of sub-networks on a specific node. For simplicity, we set sizes of sub-network sets for all nodes as a constant h. Thus, we can obtain N sets of sub-networks with the same size for brain network with N nodes, *i.e.*,

$$\mathbb{G} = \{\mathcal{G}_1^h, \mathcal{G}_2^h, \ldots, \mathcal{G}_N^h\}$$
$$\mathbb{H} = \{\mathcal{H}_1^h, \mathcal{H}_2^h, \ldots, \mathcal{H}_N^h\} \qquad (3)$$

Given a fixed d, the obtained sub-networks can be represented in a common mathematical space (*i.e.*, the space of symmetric positive semidefinite matrices $C \in R^{d \times d}$) according to Eq. (1), and thus can be compared to each other. Considering the uniqueness of each node, we can define the

---

Algorithm 1 Sub-Network Kernel Construction

Input: Two brain networks $\mathcal{G}$ and $\mathcal{H}$ (each with N nodes), and the numbers d and h

1 Step1: Construct N sets of sub-networks for each brain network by Eq. (2) and Eq. (3)

2 Step2: Compute the similarity between $\mathcal{G}_i^h$ and $\mathcal{H}_i^h$ by Eq. (5)

3 Step3: Compute the kernel $k(\mathcal{G}, \mathcal{H})$ by Eq. (4)

Output: Graph Kernel $k(\mathcal{G}, \mathcal{H})$

---

kernel on brain networks $\mathcal{G}$ and $\mathcal{H}$ by computing the similarity between pairs of sub-networks from the same node, *i.e.*,

$$k(\mathcal{G}, \mathcal{H}) = \frac{1}{N} \sum_{i=1}^{N} f(\mathcal{G}_i^h, \mathcal{H}_i^h) \qquad (4)$$

with

$$f(\mathcal{G}_i^h, \mathcal{H}_i^h) = \frac{1}{h} \sum_{j=1}^{h} g(G_i^j, H_i^j) \qquad (5)$$

and

$$g(G_i^j, H_i^j) = exp(-\frac{1}{2} \log(|A_i^j|/\sqrt{|C^{G_i^j}||C^{H_i^j}|})) \qquad (6)$$

where $|\cdot|$ denotes the determinant, $C^{G_i^j} \in R^{d \times d}$ and $C^{H_i^j} \in R^{d \times d}$ represent the corresponding covariance matrices, which are, respectively, defined on the sub-networks G_i^j and H_i^j by Eq. (1) via computing the first d terms of power iteration of their adjacency matrices, $A_i^j = (C^{G_i^j} + C^{H_i^j})/2$.

Accordingly, the function in Eq. (6) defines the similarity of a pair of sub-networks G_i^j and H_i^j by calculating Bhattacharya similarity between corresponding covariance matrices $C^{G_i^j}$ and $C^{H_i^j}$. Then, the function in Eq. (5) defines the similarity of pairs of sub-networks from the same node. Finally, the function in Eq. (4) defines the similarity of pairs of sub-networks for all nodes, which measures the similarity of brain networks $\mathcal{G}$ and $\mathcal{H}$. The detailed construction process of proposed graph kernel is summarized in Algorithm 1. Since the Bhattacharya similarity is positive semi-definite, the kernel defined in Eq. (4) is also positive semi-definite kernels according to the principle of weighted summation kernel [8]. Thus, the proposed kernel is a valid kernel, and hence can be directly used in the existing kernel-based methods, such as SVM.

It is worth noting that a set of sub-networks (*e.g.*, $\mathcal{G}_i^h$) are constructed on a particular node (*e.g.*, v_i) to reflect the multi-level topological properties of each node in a brain network, and the size for the set of sub-networks is decided by h. Intuitively, the set of sub-networks with larger value of h can reflect more global topological property (*i.e.*, containing much more nodes and edges), and $G_i^s \subseteq G_i^j$ if $s < j(s, j \in [1, \cdots, h])$). Besides, the kernel defined in Eq. (5) computes the similarity of each pair of sub-network sets constructed on each node. Therefore, our proposed graph kernel can *not only* capture the level-specific-topological properties on nodes of brain networks, *but also* take into account the uniqueness of node. Furthermore, the kernel in Eq. (5) is also a valid kernel,

which measures similarity of specific brain region across brain networks.

Computation Complexity: The complexity for constructing sub-networks is $\mathcal{O}(N^2)$. According to [11], the complexity for computing the similarity of a pair of sub-graphs (*w.r.t.* sub-networks) is $O(s_i^j d + t_i^j d^2 + d^3)$, where s_i^j and t_i^j denote the maximum number of edges and the maximum number of nodes on both sub-graphs G_i^j and H_i^j, respectively. Note that $s_i^j < S$, $t_i^j < N$, where S and N denote the numbers of edges and nodes on brain network, respectively. Thus, the total time complexity in computing the similarity of a pair of connectivity networks is less than $O(Nh(Sd + Nd^2 + d^3) + N^2)$. Finally, the total time complexity of Algorithm 1 is less than $\mathcal{O}(N(S + N) + N^2)$, since $d \ll N$ and $h \ll N$.

D. Sub-Network Kernel Based Learning

1) Discriminative Network Construction: Since the brain networks of all subjects are full-connected, for improving classification performance, we first screen out those less discriminative nodes (or brain regions) from the original brain networks and then construct more discriminative networks. Specifically, we first extract the local weighted clustering coefficient $c_i(i = 1, \cdots, N)$ [22] from the original brain connectivity network $\mathcal{G}$ with N nodes.

$$c_i = \frac{2}{d_i(d_i - 1)} \sum_{j,k=1}^{N} (w_{ij} w_{jk} w_{ki})^{1/3} \qquad (7)$$

where d_i is the number of neighboring nodes around node v_i, and w_{ij} represents the weight (*i.e.*, Pearson correlation coefficient) between node v_i and node v_j. These extracted clustering coefficients are composited as a feature vector and used for subsequent feature selection. Then, we perform a standard paired t-test to screen out features that are not significant for discrimination between patients and normal controls. For instance, given training subjects, the p-value of each feature is first computed via standard t-test and then features with p-value larger than a given threshold are considered as insignificant features and thus removed. Finally, all surviving features (*i.e.*, brain ROIs) are used to construct the discriminative network with the same weights of edges as in the original connectivity network.

2) Network Thresholding: The functional connectivity networks and the corresponding discriminative networks of all subjects are fully connected, with edge weights corresponding to the Pearson correlation coefficients. To reflect the topological properties of discriminative networks, we simultaneously threshold them with a set of predefined values using the following formulation:

$$w_{ij}^m = \begin{cases} 0, & \text{if } w_{ij} < T_m \\ 1, & \text{otherwise.} \end{cases} \qquad (8)$$

where $T = \{T_m\}_{m=1,2,\cdots,M}$ denotes a set of given thresholds, and M is the number of thresholds. In this way, the edges with zero weights will be removed. Here, we select multiple thresholds instead of a single threshold, since there is no golden standard to select the optimal threshold. Also, the brain

networks with multiple thresholds may represent multiple levels of topological properties (*i.e.*, the networks with larger threshold often preserve fewer connections and thus are sparser in connections). These properties may be complementary to each other in improving the classification performance. It is worth noting that all nodes are unchanged in network thresholding step, thus still having the same nodes (*i.e.*, ROIs) in thresholded networks for all subjects.

3) Multi-Kernel SVM Classification: We compute our proposed sub-network kernels on each thresholded network across different subjects according to Algorithm 1. Therefore, we can get multiple kernels with multiple predefined thresholds. Finally, we adopt a multi-kernel SVM technique used in [48] for classification, *i.e.*, by adopting the following multi-kernel learning technique to combine the multiple graph kernels:

$$k(\mathcal{G}, \mathcal{H}) = \sum_{m=1}^{M} \alpha_m k_m(\mathcal{G}, \mathcal{H}) \qquad (9)$$

where $k_m(\mathcal{G}, \mathcal{H})$ denotes the kernel function over the m-th thresholded networks across brain networks $\mathcal{G}$ and $\mathcal{H}$, and α_m is a no-negative weight parameter with $\sum_{m=1}^{M} \alpha_m = 1$. Following work in [48], we adopt a coarse-grid search approach via cross-validation on the training subjects to determine the optimal α_m. Once the optimal parameter $\alpha_m (m = 1, 2, \cdots, M)$ is obtained, multiple kernels will be transform into single kernel, so traditional SVM technique can be directly applied for classification.

IV. RESULTS

In this section, we present our experimental settings, results of brain disease classification and comparison between our proposed method and several state-of-the-art network-based methods.

A. Methods for Comparison

We compare our proposed sub-network kernels to the state-of-the-art kernels that are selected to represent three major groups of graph kernels, *i.e.*, defined on subtrees, shortest paths, and edges, respectively. Those graph kernels belong to the Weisfeiler-Lehman graph kernel framework proposed in [43] (thus denoted as WL-subtree, WL-shortestpath and WL-edge, respectively, in this paper). Also, we compare with the graph kernels defined in [11] for measuring the similarity of ego network (denoted as Ego-net in this paper) and shortest-path kernels proposed in [40] (denoted as Shortest-path in this paper). It is worth noting that all graph kernels used for comparison are constructed by ignoring the label information of nodes in the brain networks. Besides, we also compare with the baseline method using only local topological measures (*i.e.*, weighted clustering coefficients [22]) as features, where t-test is used for feature selection and a linear SVM is used to perform classification.

B. Experimental Setting

In our experiments, two kinds of binary classification tasks are performed, *i.e.*, 1) MCI vs. NC classification, and

TABLE II
CLASSIFICATION RESULTS OF ALL METHODS. ACC: ACCURACY, BAC: BALANCED ACCURACY

Method	MCI vs. NC			EMCI vs. LMCI		
	ACC(%)	BAC(%)	AUC	ACC(%)	BAC(%)	AUC
Baseline	65.1	51.5	0.51	55.6	50.0	0.55
Ego-net	73.2	61.0	0.62	62.6	58.6	0.58
Shortest-path	72.5	64.0	0.67	63.6	61.9	0.63
WL-edge	69.1	62.9	0.64	65.7	64.0	0.66
WL-subtree	76.5	67.5	0.73	70.7	67.4	0.70
WL-shortestpath	63.1	57.4	0.61	64.6	63.1	0.62
SKL	**82.6**	**75.5**	**0.78**	**74.8**	**72.6**	**0.72**

2) early MCI (EMCI) vs. late MCI (LMCI) classification. We evaluate the classification performance using the leave-one-out (LOO) cross-validation with a SVM classifier. The performances of all methods are evaluated by computing the classification accuracy, balanced accuracy (*i.e.*, the average accuracy obtained on either class), and area under receiver operating characteristic (ROC) curve (AUC).

In our study, The SVM is implemented based on the LIBSVM library [49] with the default parameter values. A statistical t-test with the same threshold (*i.e.*, p-value < 0.01) is performed to construct the discriminative network. For simplicity, we adopt five different values (*i.e.*, $T = \{0.30, 0.35, 0.40, 0.45, 0.50\}$) to threshold the obtained discriminative networks. The corresponding average connection density (*i.e.*, the fraction of present connections to all possible connections) of each threshold is located in the interval [30%, 70%]. It has been reported that the average connection density interval of [25%, 75%] demonstrates higher classification performance [28]. In the classification step, the optimal parameter α_m is learned based on another LOO cross-validation on the training subjects via a grid search, using the range from 0 to 1 with step size of 0.1.

C. Classification Performance

Classification results of all methods are summarized in Table II. For comparison, in Fig. 5, we also give the classification performances of different methods under different single thresholded sub-networks. As shown in Table II, our proposed method consistently outperforms other methods in both classification tasks. Specifically, our proposed method yields accuracies of 82.6% and 74.8% for MCI vs. NC and EMCI vs. LMCI classification, respectively, while the best accuracies of the competing methods are 76.5% and 70.7%, respectively. Also, our proposed method yields balanced accuracies of 75.5% and 72.6% in both classification tasks, respectively, while the best balanced accuracies of other methods are 67.5% and 67.4%, respectively. In addition, the AUC of proposed method, respectively, is 0.78 and 0.72 in two tasks, which indicates excellent diagnostic power. Besides, we could observe from Fig. 5 that 1) the combination of multiple thresholded networks performs significantly better than the method using any single thresholded network alone, and 2) the performance of our graph kernel on single thresholded network
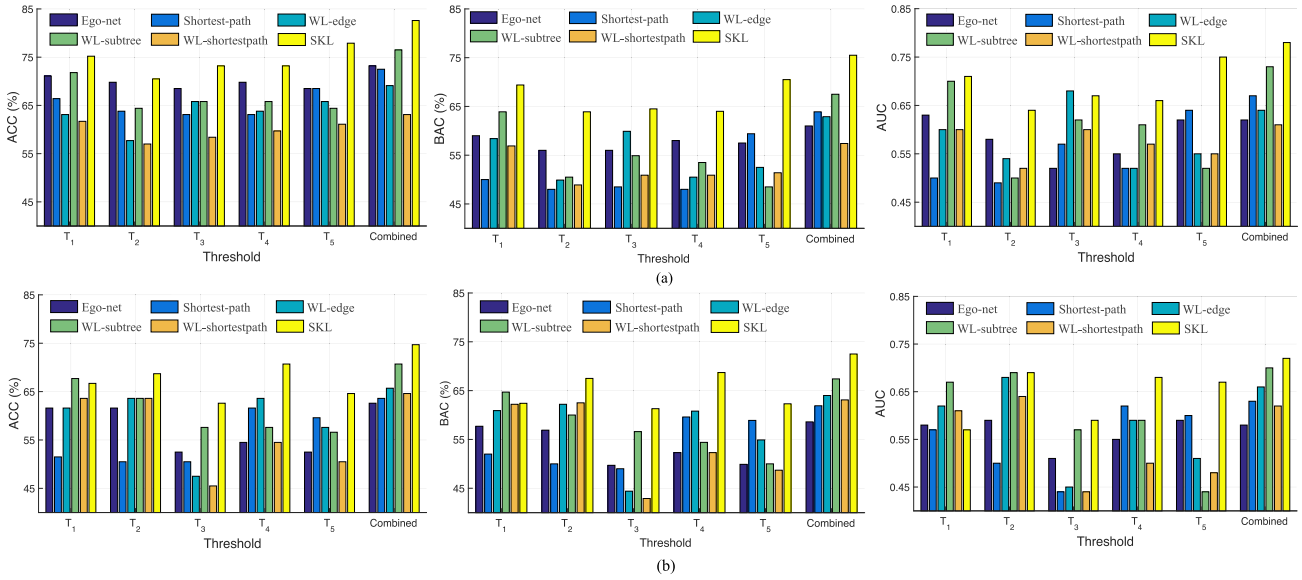
Fig. 5. Classification performances of different methods with single or multiple thresholed network, in (a) MCI vs. NC classification, and (b) EMCI vs. LMCI classification. Here, T_1, T_2, T_3, T_4, and T_5 denote using the single thresholded network, respectively, while "combined" denotes using all thresholded networks.

also outperforms the performances of the state-of-the-art graph kernels, which again shows the efficacy of our proposed graph kernel.

In addition, for better comparison, we also test the performance of AD vs. NC and AD vs. MCI classifications with the same experiment setting. Table S3 in the Supporting Information gives the results of all methods. As we can see from Table S3, the proposed method consistently performed better than the competing methods for AD vs. NC and AD vs. MCI classifications, which further demonstrates the efficacy of our proposed method.

D. Discriminative Power of Proposed Graph Kernels

In this subsection, we investigate the discriminative power of our proposed graph kernels. In the step of constructing discriminative networks, since the training subjects are slightly different in different LOO cross-validation folds, and the selected ROIs by t-test based feature selection are often different, thus the corresponding constructed discriminative networks are also different. Therefore, we first construct a common discriminative network from the original connectivity network of each subject, with its nodes corresponding to the ROIs occurred in all LOO cross-validations while its weights corresponding to those in the original connectivity network. Then, we use the same thresholds as used in the classification step to simultaneously threshold this common discriminative sub-network. Finally, based on each thresholded common discriminative sub-network, we perform a significance test between two groups of graph kernels, *i.e.*, the graph kernels constructed on intra-class subjects (*i.e.*, subjects with the same class label) and the graph kernels constructed on inter-class subjects (*i.e.*, subjects with the different class label), using the standard paired t-test.

The obtained p-values for the five thresholded common discriminative networks are 2.39×10^{-4}, 1.22×10^{-8},

2.04×10^{-3}, 2.31×10^{-10} and 7.76×10^{-5}, respectively. These results show the values of graph kernel constructed on intra-class subjects are significantly larger than those defined on inter-class subjects (*i.e.*, with very small corresponding p-values), which indicates our proposed graph kernels can capture the topological similarity of brain networks for brain disease classification.

E. Important Brain Regions

Furthermore, in this subsection, we investigate the importance of ROIs (*i.e.*, brain regions) based on our proposed graph kernel. Since the kernel defined in Eq. 5 measures the similarity of each ROI across brain networks, we can identify some important brain regions according to their classification performance using this kernel. Specifically, we also construct the common discriminative network from all LOO cross-validations using the same approach as described in the above subsection, and simultaneously threshold this network with the same five different thresholds. Then, for each thresholded network, we construct the kernels on each ROI among sub-network sets from that ROI across brain networks according to Eq. 5, and compute the accuracy of each ROI for MCI classification with SVM classifier via a LOO cross-validation strategy. Finally, we rank these ROIs according to their classification accuracy and select the top 10 ROIs with the highest classification accuracy. Table S2 in the *Supporting Information* gives those ROIs selected from each thresholded networks. Figure 6 also shows all those ROIs. These selected ROIs include hippocampus, cingulate, parahippocampal gyrus, amygdala, heschl gyrus and temporal gyrus, which are consistent with those reported in that previous studies.

F. Connectivity Analysis

To analyze the connectivities between those selected ROIs in the above section and to visually show the differences
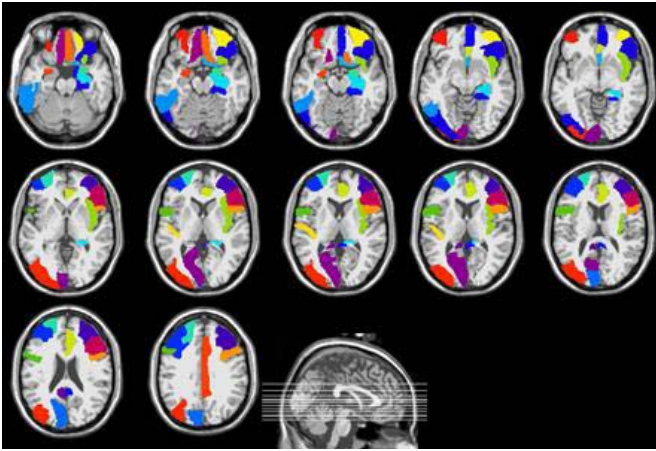
Fig. 6.   The important ROIs selected by our proposed sub-network kernel.
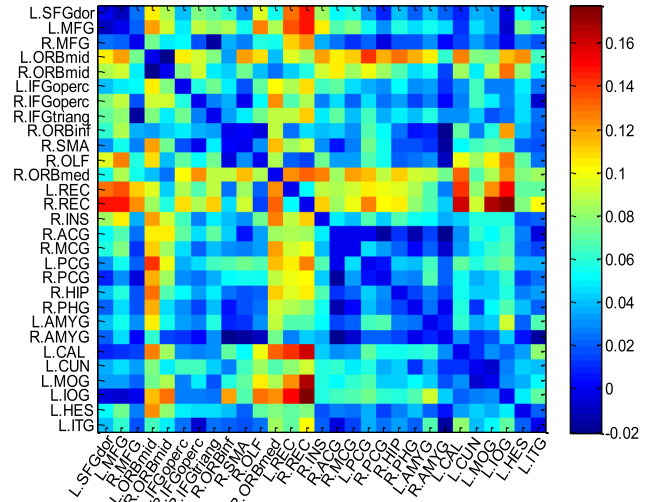

Fig. 7.   Difference in average connectivity networks based on all selected ROIs between NC and MCI groups. Here, colors denote the amounts of difference between two groups on different pairs of ROIs.

on connectivity networks for patients and normal controls, we also compute the average network based on all selected ROIs in Fig. 6. Specifically, for each group (*i.e.*, MCI patients or normal controls), we define an average network based on all selected ROIs with each connection as the average of connectivity strength of corresponding edge in the original brain networks for subjects from the same group, and compute the connectivity difference between patient group and normal control (NC) group. Fig. 7 graphically shows the obtained results, where color in Fig. 8 denote the difference of connectivity strength. As we can see from Fig. 7, the connectivity strengths in MCI group are lower than those in NC group in almost all cases. This result is consistent with previous findings using group analysis method. On the other hand, to visualize the topology of connectivity network for MCI and NC, we construct a thresholded average connectivity sub-network from the average connectivity network of each group, based on the ROIs selected in each thresholded network (listed in Table S2 in *Supporting Information*). For instance, the ROIs selected in each thresholded network are used to define an average connectivity network with the nodes corresponding to the selected ROIs and the connections corresponding to the connections in the average connectivity network of each group, and the value used for thresholding the discriminative connectivity networks is also used to threshold this average connectivity sub-network. Fig. 8 plots those thresholded average connectivity sub-networks. Here, T_1, T_2, T_3, T_4, T_5 denote the single thresholded average connectivity sub-networks, respectively. Each node in Fig. 8 represents an ROI, and each edge in Fig. 8(a)-(b) represents the connectivity between each pair of ROIs. While, each edge in Fig. 8(c) denotes the changed connectivity between MCI and NC groups, with blue edges and red edges denoting the decreasing and increasing functional connectivity in MCI patient, respectively. As can be seen from Fig. 8, compared with NC group, the connections in MCI group are significantly reduced, which again suggests possible disruption in connectivity between those ROIs, as reported in the previous studies.

V. DISCUSSION

In this paper, we have proposed a novel sub-network kernel for similarity computation of brain networks. The key of our

proposed kernel is to take into account the inherent characteristics of brain network and capture the multi-level topological properties on nodes of brain networks. Furthermore, we built a sub-network kernel based learning framework for MCI classification. We have evaluated the performance of our proposed method on a real MCI dataset from ADNI via LOO cross-validation to ensure the generalization of the classifier. The experimental results show that, compared with the state-of-the-art graph kernels, our proposed sub-network kernel can significantly improve brain disease classification performance, thus can be potentially used for automated image-based classification of brain diseases. In addition, based on proposed graph kernel, we have identified disease-related brain regions and found that these brain regions are related with MCI disease and have been widely reported in the previous studies. It is worth noting that our proposed graph kernel is a general similarity measure for brain networks, which can also be applied to other similarity-based brain network analysis tasks, such as the regression/prediction of some clinical scores (*e.g.*, MMSE).

A. Significance of Results

Graph objects have been widely used for brain network analysis (*e.g.*, classification). In the graph-based network analysis method, a fundamental challenge task is how to compute the similarity of a pair of graphs (*i.e.*, networks). Among all kinds of methods, kernel methods provide a general framework to solve this problem. However, existing graph kernels mainly focus on general graphs and thus ignore some specific characteristics of brain network. In this paper, we have built a novel brain-network-oriented kernel and applied it to brain disease classification. The experimental results on a real MCI dataset show the efficiency of our proposed method, compared with the state-of-the-art methods.

In addition, some important ROIs have been identified based on our proposed graph kernel. These ROIs include hippocampus [14], [50], cingulate [50], [51], parahippocampal
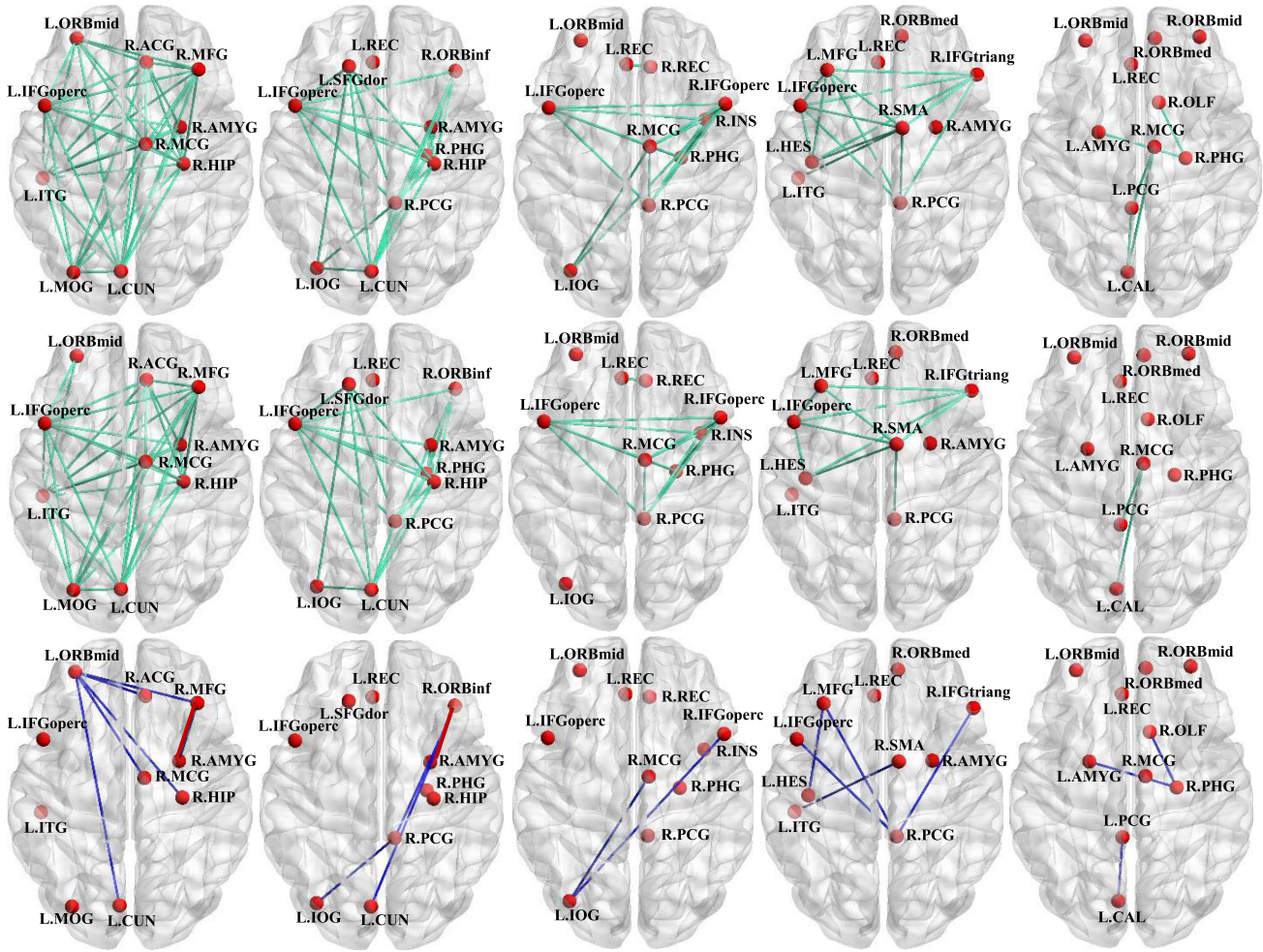
Fig. 8. Illustration of thresholded average connectivity networks with selected ROIs (listed in Table S2 in the *Supporting Information*) for (a) top row: NC group and (b) middle row: MCI group, along with (c) bottom row: their group difference of thresholded average connectivity network. Here, red nodes denote brain regions, the connections in (a) and (b) denote the connectivities between brain regions. While the connections with different colors in (c) denote increase (red connection) or decrease (blue connection) of functional connectivity in MCI patients, compared with NC group.

gyrus [10], amygdala [51], heschl gyrus [52] and temporal gyrus [53], which have been reported in the previous MCI studies. For example, hippocampal formation is one of the first brain regions to suffer damage with memory loss and disorientation. It is widely reported that the hippocampal formation is damaged heavily in early AD and MCI [14], [50], and is a focal point for pathology [54]. The amygdala, as another important subcortical region, is one of the most vulnerable structures in the early stage of AD. Studies have reported the alteration of the functional connectivity of the amygdala in MCI patients [55].

Further analysis of connectivity between identified brain regions shows that the connectivity strengths in MCI group are lower than those in NC group in almost all cases, which is also consistent with the previous studies using group analysis method. For example, Wang *et al.* [24] have found disrupted functional connectivity between different functional modules by investigating functional connectome of MCI patients. Bai *et al.* [56] also found the evidence of impaired connectivity in the MCI group by exploring the properties of whole-brain networks. Other studies have found a loss of small-world

characteristics in AD/MCI patients [9], [15], [52]. Besides, a series of abnormal connectivities have been reported in both EMCI and LMCI [57], [58].

These changes may suggest that the connectivities between some brain regions are disrupted by the disease. These results may also suggest that these disrupted connectivities may lead to reduced functional integration and information processing capability of the brain, which may account for cognitive deficits in patients. On the other hand, these changes also provide an important alternative to explore the properties of brain connectivity network for classification of brain diseases. Our results demonstrate that the proposed method can effectively classify MCI from NC, and classify LMCI from EMCI, by making use of topological properties of functional connectivity networks, which also provides empirical evidence for disrupted network organization in MCI (including EMCI and LMCI) patients.

B. Effect of Parameters

In our proposed graph kernel, there are two parameters, *i.e.*, the numbers d and h. The number d controls the number
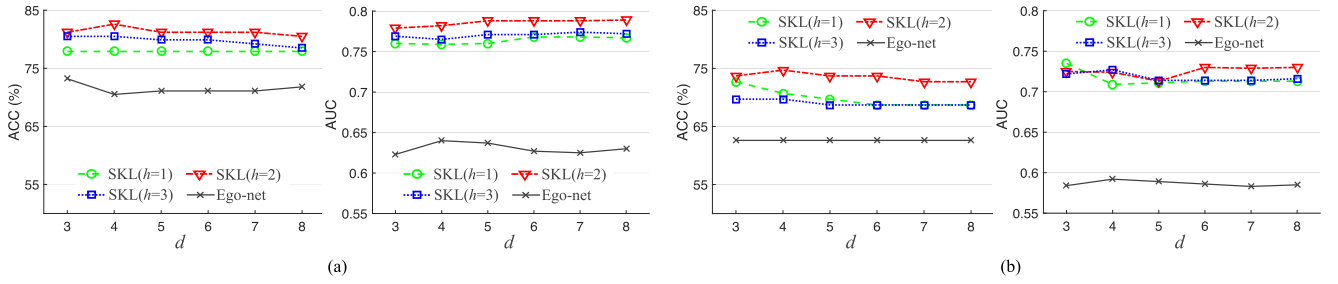
Fig. 9. The classification performance of our proposed method using different parameters (*i.e.*, *d* and *h*) in (a) MCI vs. NC classification, and (b) EMCI vs. LMCI classification.

of algorithm iterations in computing the mathematical representation of sub-networks. The number *h* controls the size of a sub-network set. To investigate the effects of these two parameters on the classification performance of our proposed graph kernel, we test different values for the number *d* from $\{3, 4, 5, 6, 7, 8\}$, and also the number *h* from $\{1, 2, 3\}$. Fig. 9 shows the classification results *with respect to* different values of the numbers *d* and *h*. For comparison, in Fig. 9 we also give the classification performance of Ego-net method proposed in [11] with different values of *d* (*i.e.*, $d = \{3, 4, 5, 6, 7, 8\}$). As we can see from Fig. 9 and Table II, for all parameter values, our proposed method significantly outperforms the Ego-net method on both classification tasks. Also, for most values of *d* and *h*, the classification performance of our defined graph kernel outperforms the performances of other graph kernels, which further shows the efficacy of our graph kernel. Besides, Fig. 9 shows that, with a fixed *h*, the curves varied with the value of *d* are very smooth, which shows that our method is very robust to the parameter *d*. Moreover, from Fig. 9 we can observe that, given a fixed *d*, the classification performance is largely affected by different values of *h*. When $h = 2$, our graph kernel obtains the best classification performance. These results imply that the selection of *h* is critical for our proposed graph kernel. This is reasonable since the number *h* controls the size of a sub-network set for each node in a brain network, and thus affects the similarity measurement of brain networks.

C. Influence of Different Brain Network Modeling Methods

A number of modeling methods have been proposed for estimating the functional connectivity networks, with the varying degrees of validation [59]. To evaluate the robustness of our method for different network modeling methods, we test the classification performance of our proposed graph kernels by using sparse inverse covariance estimation (SICE) [60], also called Gaussian graphical model, for brain network estimation. Specifically, for each subject, we use the resulting sparse inverse covariance matrix $\hat{\Theta}$ from SICE to build connectivity network, where edges correspond to the conditional partial correlation between nodes (*i.e.*, ROIs). That is, if $\hat{\Theta}_{ij} = 0$, then ROIs *i* and *j* are conditionally independent, and there is no edge between them (*i.e.*, $W_{ij} = 0$); otherwise, $W_{ij} = 1$. Since the regularization parameter λ in SICE controls the sparsity of inverse covariance matrix $\hat{\Theta}$, we simultaneously use five different values of λ (*i.e.*, $\lambda = \{0.2, 0.3, 0.4, 0.5, 0.6\}$) to build five brain networks with different connection densities.

Then, we directly compute the proposed graph kernels on the brain networks constructed with each λ value across different subjects, and use the multi-kernel SVM technique defined in Eq. 9 for classification. Table S4 in the Supporting Information gives the classification results of our proposed graph kernel.

The results show that our proposed graph kernel, respectively, yields accuracies of 83.2% and 73.7% for MCI vs. NC and EMCI vs. LMCI classifications, indicating the robustness of our proposed graph kernel for different brain network modeling methods. In addition, for comparison, Table S4 also gives the classification performance of other graph kernels, including Ego-net, Shortest-path, WL-subtree, WL-shortestpath and WL-edge. These results further demonstrate the efficacy of our proposed method.

D. Effect of Discriminative Networks

In the proposed SKL framework, we construct the discriminative networks from the original functional connectivity networks for improving the classification performance. In order to evaluate the effect of this step, we test the performance of our proposed SKL framework without constructing the discriminative networks. Specifically, we directly threshold the original functional connectivity networks derived from rs-fMRI data using the same five different thresholds, and further construct five sub-network kernels and perform the multi-kernel SVM classification. Table S5 in the Supporting Information gives the classification results of our proposed graph kernel. As we can see from Table II and Table S5, the results of the proposed SKL using discriminative networks are better than those of the method without using discriminative networks, indicating the importance of constructing discriminative networks. For comparison, Table S5 also gives the classification performance of other methods without using discriminative networks, including Ego-net, Shortest-path, WL-subtree, WL-shortestpath and WL-edge. The results show that, compared with the competing methods, our proposed graph kernel still achieves the best performance, indicating again the efficacy of our proposed method.

E. Importance of Network Topology

In our studies, the sub-network-based topological properties are used to construct the graph kernel for measuring the similarity of brain networks. To evaluate the importance of topological properties of network, we do another experiment

to test the classification performance by directly using the adjacency matrices of brain networks. Specifically, we convert the adjacency matrix of functional connectivity network derived from rs-fMRI into a vector, followed by *t*-test for feature selection and a linear SVM for classification. In both tasks of MCI vs. NC classification and EMCI vs. LMCI classification, this achieves accuracies of 59.7% and 53.5%, respectively. These results are inferior to those of graph-kernel-based methods (see Table II and Fig. 5), suggesting that the topological properties of networks help improve the performance of brain disease classification.

F. Limitation

Currently, this study is limited by the following four aspects. First, more priori knowledge about brain disease may be embed into network similarity measurement to improve the learning performance. For instance, there may have different effects on different brain regions by a specific brain disease, thus different brain regions should have their own importance for network similarity measurement, which is not considered in current studies. Second, the definition of nodes (*i.e.*, brain parcellation) is a very important step for brain network analysis. Existing studies have shown that the connectivity networks constructed with different brain parcellations exhibit different topological properties [61], while our current work did not analyze the effects of different brain parcellations on the performance of our proposed method. Third, we construct the graph kernel by comparing the similarity of sub-networks. However, the label information of nodes in sub-networks is ignored in our proposed method, considering that those sub-networks usually have different topologies (*i.e.*, containing different nodes and edges). It is very interesting to explore label information for further improving the performance of graph kernels. Finally, there are only 183 studied subjects used in the experiments. In the future work, we will further evaluate our proposed method on a larger size of dataset.

VI. CONCLUSIONS

The similarity measurement between graphs (or networks) is a fundamental challenge in network-based analysis. In this paper, we have built a novel sub-network kernel for measuring the similarity of a pair of brain networks. Different from existing graph kernels, our constructed graph kernels can effectively reflect the specific characteristics of brain networks and also capture multi-level topological properties of each node in brain networks. We have further developed a sub-network kernel based learning framework for MCI classification using rs-fMRI data, with the experimental results demonstrating the efficacy of our proposed method.

REFERENCES

[1] R. C. Petersen *et al.*, "Current concepts in mild cognitive impairment," *Arch. Neurol.*, vol. 58, no. 12, pp. 1985–1992, 2001.
[2] O. Sporns, "Contributions and challenges for network models in cognitive neuroscience," *Nature Neurosci.*, vol. 17, no. 5, pp. 652–660, 2014.
[3] O. A. Sporns, "From simple graphs to the connectome: Networks in neuroimaging," *NeuroImage*, vol. 62, no. 2, pp. 881–886, 2012.
[4] M. Liu, J. Zhang, E. Adeli, and D. Shen, "Landmark-based deep multi-instance learning for brain disease diagnosis," *Med. Image Anal.*, vol. 43, pp. 157–168, Jan. 2018.
[5] M. R. Brier *et al.*, "Functional connectivity and graph theory in preclinical Alzheimer's disease," *Neurobiol. Aging*, vol. 35, no. 4, pp. 757–768, 2014.
[6] B. M. Tijms *et al.*, "Alzheimer's disease: Connecting findings from graph theoretical studies of brain networks," *Neurobiol. Aging*, vol. 34, no. 8, pp. 2023–2036, 2013.
[7] C.-Y. Wee *et al.*, "Identification of MCI individuals using structural and functional connectivity networks," *NeuroImage*, vol. 59, no. 3, pp. 2045–2056, 2012.
[8] B. Schölkopf and A. J. Smola, *Learning With Kernels: Support Vector Machines, Regularization, Optimization, and Beyond*. Cambridge, MA, USA: MIT Press, 2002.
[9] E. J. Sanz-Arigita *et al.*, "Loss of 'small-world' networks in Alzheimer's disease: Graph analysis of fMRI resting-state functional connectivity," *PLoS ONE*, vol. 5, no. 11, p. e13788, 2010.
[10] J. Soldner *et al.*, "Structural and functional neuronal connectivity in Alzheimer's disease: A combined DTI and fMRI study," *Der Nervenarzt*, vol. 83, no. 7, pp. 878–887, 2012.
[11] A. Shrivastava and P. Li, "A new space for comparing graphs," in *Proc. IEEE/ACM Int. Conf. Adv. Social Netw. Anal. Mining (ASONAM)*, Aug. 2014, pp. 62–71.
[12] E. Bullmore and O. Sporns, "Complex brain networks: Graph theoretical analysis of structural and functional systems," *Nature Rev. Neurosci.*, vol. 10, no. 3, pp. 186–198, Mar. 2009.
[13] M. Kaiser, "A tutorial in connectome analysis: Topological and spatial features of brain networks," *NeuroImage*, vol. 57, no. 3, pp. 892–907, 2011.
[14] F. Bai *et al.*, "Abnormal functional connectivity of hippocampus during episodic memory retrieval processing network in amnestic mild cognitive impairment," *Biol. Psychiatry*, vol. 65, no. 11, pp. 951–958, 2009.
[15] K. Supekar, V. Menon, D. Rubin, M. Musen, and M. D. Greicius, "Network analysis of intrinsic functional brain connectivity in Alzheimer's disease," *PLoS Comput. Biol.*, vol. 4, no. 6, p. e1000100, 2008.
[16] M. D. Greicius, G. Srivastava, A. L. Reiss, and V. Menon, "Default-mode network activity distinguishes Alzheimer's disease from healthy aging: Evidence from functional MRI," *Proc. Nat. Acad. Sci. USA*, vol. 101, no. 13, pp. 4637–4642, 2004.
[17] J. A. Brown *et al.*, "Brain network local interconnectivity loss in aging APOE-4 allele carriers," *Proc. Nat. Acad. Sci. USA*, vol. 108, no. 51, pp. 20760–20765, 2011.
[18] M. R. Arbabshirani, K. A. Kiehl, G. D. Pearlson, and V. D. Calhoun, "Classification of schizophrenia patients based on resting-state functional network connectivity," *Frontiers Neurosci.*, vol. 7, p. 133, Jul. 2013.
[19] M. Guye, G. Bettus, F. Bartolomei, and P. J. Cozzone, "Graph theoretical analysis of structural and functional connectivity MRI in normal and pathological brain networks," *Magn. Reson. Mater. Phys., Biol. Med.*, vol. 23, nos. 5–6, pp. 409–421, 2010.
[20] B. Jie, D. Zhang, W. Gao, Q. Wang, C.-Y. Wee, and D. Shen, "Integration of network topological and connectivity properties for neuroimaging classification," *IEEE Trans. Biomed. Eng.*, vol. 61, no. 2, pp. 576–589, Feb. 2014.
[21] C.-Y. Wee *et al.*, "Disrupted brain functional network in Internet addiction disorder: A resting-state functional magnetic resonance imaging study," *PLoS ONE*, vol. 9, no. 9, p. e107306, 2014.
[22] M. Rubinov and O. Sporns, "Complex network measures of brain connectivity: Uses and interpretations," *NeuroImage*, vol. 52, no. 3, pp. 1059–1069, 2010.
[23] S. Achard and E. Bullmore, "Efficiency and cost of economical brain functional networks," *PLoS Comput. Biol.*, vol. 3, no. 2, p. e17, 2007.
[24] J. Wang *et al.*, "Disrupted functional brain connectome in individuals at risk for Alzheimer's disease," *Biol. Psychiatry*, vol. 73, no. 5, pp. 472–481, Mar. 2013.
[25] B. Jie, C.-Y. Wee, D. Shen, and D. Zhang, "Hyper-connectivity of functional networks for brain disease diagnosis," *Med. Image Anal.*, vol. 32, pp. 84–100, Aug. 2016.
[26] G. Chen *et al.*, "Classification of Alzheimer disease, mild cognitive impairment, and normal cognitive status with large-scale network analysis based on resting-state functional MR imaging," *Radiology*, vol. 259, no. 1, pp. 213–221, 2011.
[27] C.-Y. Wee *et al.*, "Enriched white matter connectivity networks for accurate identification of MCI patients," *NeuroImage*, vol. 54, no. 3, pp. 1812–1822, 2011.

[28] M. Zanin *et al.*, "Optimizing functional network representation of multivariate time series," *Sci. Rep.*, vol. 2, p. 630, Sep. 2012.

[29] B. Jie, D. Zhang, B. Cheng, and D. Shen, "Manifold regularized multitask feature learning for multimodality disease classification," *Human Brain Mapping*, vol. 36, no. 2, pp. 489–507, 2015.

[30] F. Mokhtari, S. K. Bakhtiari, G. A. Hossein-Zadeh, and H. Soltanian-Zadeh, "Discriminating between brain rest and attention states using fMRI connectivity graphs and subtree SVM," *Proc. SPIE*, vol. 8314, pp. 83144C.1–83144C.7, Feb. 2012.

[31] D. Shahnazian, F. Mokhtari, and G.-A. Hossein-Zadeh, "A method based on the Granger causality and graph kernels for discriminating resting state from attentional task," in *Proc. Int. Conf. Biomed. Eng. (ICoBE)*, 2012, pp. 83–88.

[32] M. Liu, D. Zhang, S. Chen, and H. Xue, "Joint binary classifier learning for ECOC-based multi-class classification," *IEEE Trans. Pattern Anal. Mach. Intell.*, vol. 38, no. 11, pp. 2335–2341, Nov. 2016.

[33] G. Camps-Valls, N. Shervashidze, and K. M. Borgwardt, "Spatio-spectral remote sensing image classification with graph kernels," *IEEE Geosci. Remote Sens. Lett.*, vol. 7, no. 4, pp. 741–745, Oct. 2010.

[34] Y. Zhang, H. Lin, Z. Yang, and Y. Li, "Neighborhood hash graph kernel for protein–protein interaction extraction," *J. Biomed. Inform.*, vol. 44, no. 6, pp. 1086–1092, 2011.

[35] B. Jie, D. Zhang, C.-Y. Wee, and D. Shen, "Topological graph kernel on multiple thresholded functional connectivity networks for mild cognitive impairment classification," *Human Brain Mapping*, vol. 35, no. 7, pp. 2876–2897, 2014.

[36] F. Liu *et al.*, "Multivariate classification of social anxiety disorder using whole brain functional connectivity," *Brain Struct. Funct.*, vol. 220, no. 1, pp. 101–115, Jan. 2015.

[37] M. Liu, D. Zhang, and D. Shen, "Relationship induced multi-template learning for diagnosis of Alzheimer's disease and mild cognitive impairment," *IEEE Trans. Med. Imag.*, vol. 35, no. 6, pp. 1463–1474, Jun. 2016.

[38] D. Haussler, "Convolution kernels on discrete structures," Dept. Comput. Sci., Univ. California Santa Cruz, Santa Cruz, CA, USA, 1999.

[39] T. Gärtner, P. Flach, and S. Wrobel, "On graph kernels: Hardness results and efficient alternatives," in *Learning Theory and Kernel Machines*. Berlin, Germany: Springer, 2003, pp. 129–143.

[40] K. M. Borgwardt and H.-P. Kriegel, "Shortest-path kernels on graphs," in *Proc. 5th IEEE Int. Conf. Data Mining*, Nov. 2005, p. 8.

[41] A. Feragen, N. Kasenburg, J. Petersen, M. de Bruijne, and K. Borgwardt, "Scalable kernels for graphs with continuous attributes," in *Proc. Adv. Neural Inf. Process. Syst.*, 2013, pp. 216–224.

[42] F. D. Johansson, V. Jethava, D. Dubhashi, and C. Bhattacharyya, "Global graph kernels using geometric embeddings," in *Proc. 31st Int. Conf. Mach. Learn. (ICML)*, Beijing, China, Jun. 2014, 2014.

[43] N. Shervashidze, P. Schweitzer, E. J. van Leeuwen, K. Mehlhorn, and K. M. Borgwardt, "Weisfeiler-lehman graph kernels," *J. Mach. Learn. Res.*, vol. 12, pp. 2539–2561, Sep. 2011.

[44] S. V. N. Vishwanathan, N. N. Schraudolph, I. R. Kondor, and K. M. Borgwardt, "Graph kernels," *J. Mach. Learn. Res.*, vol. 11, pp. 1201–1242, Mar. 2010.

[45] D. Zhu *et al.*, "DICCCOL: Dense individualized and common connectivity-based cortical landmarks," *Cerebral Cortex*, vol. 23, no. 4, pp. 786–800, 2012.

[46] K. R. Van Dijk, T. Hedden, A. Venkataraman, K. C. Evans, S. W. Lazar, and R. L. Buckner, "Intrinsic functional connectivity as a tool for human connectomics: Theory, properties, and optimization," *J. Neurophysiol.*, vol. 103, no. 1, pp. 297–321, 2010.

[47] N. Tzourio-Mazoyer *et al.*, "Automated anatomical labeling of activations in SPM using a macroscopic anatomical parcellation of the MNI MRI single-subject brain," *NeuroImage*, vol. 15, no. 1, pp. 273–289, 2002.

[48] D. Zhang, Y. Wang, L. Zhou, H. Yuan, and D. Shen, "Multimodal classification of Alzheimer's disease and mild cognitive impairment," *NeuroImage*, vol. 55, no. 3, pp. 856–867, 2011.

[49] C.-C. Chang and C.-J. Lin, "LIBSVM: A library for support vector machines," *ACM Trans. Intell. Syst. Technol.*, vol. 2, no. 3, pp. 27:1–27:27, 2011.

[50] Y. Zhou, J. H. Dougherty, Jr., K. F. Hubner, B. Bai, R. L. Cannon, and R. K. Hutson, "Abnormal connectivity in the posterior cingulate and hippocampus in early Alzheimer's disease and mild cognitive impairment," *Alzheimer's Dementia*, vol. 4, no. 4, pp. 265–270, 2008.

[51] C. Davatzikos, P. Bhatt, L. M. Shaw, K. N. Batmanghelich, and J. Q. Trojanowski, "Prediction of MCI to AD conversion, via MRI, CSF biomarkers, and pattern classification," *Neurobiol. Aging*, vol. 32, no. 12, pp. 2322.e19–2322.e27, Dec. 2011.

[52] Z. Liu *et al.*, "Altered topological patterns of brain networks in mild cognitive impairment and Alzheimer's disease: A resting-state fMRI study," *Psychiatry Res., Neuroimag.*, vol. 202, no. 2, pp. 118–125, 2012.

[53] Y. Han *et al.*, "Frequency-dependent changes in the amplitude of low-frequency fluctuations in amnestic mild cognitive impairment: A resting-state fMRI study," *NeuroImage*, vol. 55, no. 1, pp. 287–295, 2011.

[54] G. W. Van Hoesen and B. T. Hyman, "Hippocampal formation: Anatomy and the patterns of pathology in Alzheimer's disease," *Prog. Brain Res.*, vol. 83, pp. 445–457, 1990.

[55] H. Yao *et al.*, "Decreased functional connectivity of the amygdala in Alzheimer's disease revealed by resting-state fMRI," *Eur. J. Radiol.*, vol. 82, no. 9, pp. 1531–1538, Sep. 2013.

[56] F. Bai *et al.*, "Abnormal whole-brain functional connection in amnestic mild cognitive impairment patients," *Behav. Brain Res.*, vol. 216, no. 2, pp. 666–672, 2011.

[57] P. Liang *et al.*, "Altered amplitude of low-frequency fluctuations in early and late mild cognitive impairment and Alzheimer's disease," *Current Alzheimer Res.*, vol. 11, no. 4, pp. 389–398, 2014.

[58] H. Yao *et al.*, "Longitudinal alteration of amygdalar functional connectivity in mild cognitive impairment subjects revealed by resting-state FMRI," *Brain Connectivity*, vol. 4, no. 5, pp. 361–370, 2014.

[59] S. M. Smith *et al.*, "Network modelling methods for FMRI," *NeuroImage*, vol. 54, no. 2, pp. 875–891, 2011.

[60] S. Huang *et al.*, "Learning brain connectivity of Alzheimer's disease by sparse inverse covariance estimation," *NeuroImage*, vol. 50, no. 3, pp. 935–949, 2010.

[61] A. Zalesky *et al.*, "Whole-brain anatomical networks: Does the choice of nodes matter?" *NeuroImage*, vol. 50, no. 3, pp. 970–983, 2010.

Biao Jie received the M.S. degree in computer science from the Yunnan Normal University, Yunnan, China, in 2006, and the Ph.D. degree in computer science from the Nanjing University of Aeronautics and Astronautics, China, in 2015. He joined the Department of Computer Science and Technology, Anhui Normal University, in 2006, where he is currently an Associate Professor. His research interests include machine learning and medical image analysis.
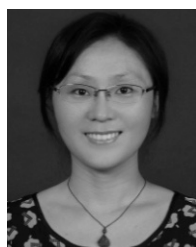
Mingxia Liu received the B.S. and M.S. degrees from Shandong Normal University, Shandong, China, in 2003 and 2006, respectively, and the Ph.D. degree from the Nanjing University of Aeronautics and Astronautics, Nanjing, China, in 2015. Her current research interests include machine learning, pattern recognition, and neuroimaging analysis.
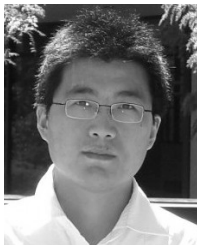
Daoqiang Zhang received the B.S. and Ph.D. degrees in computer science from the Nanjing University of Aeronautics and Astronautics (NUAA), China, in 1999 and 2004, respectively. He joined the Department of Computer Science and Engineering, NUAA, as a Lecturer in 2004, where he is currently a Professor. His research interests include machine learning, pattern recognition, data mining, and medical image analysis. In these areas, he has published over 150 scientific articles in refereed international journals, such as the IEEE TRANSACTIONS PAMI, the IEEE TRANSACTIONS MEDICAL IMAGING, the *Neuroimage*, the *Human Brain Mapping*, the *Medical Image Analysis*, and conference proceedings, such as IJCAI, AAAI, NIPS, CVPR, MICCAI, with over 8000 citations by the Google Scholar. He was nominated for the National Excellent Doctoral Dissertation Award of China in 2006, received the best paper award or the best student award of several international conferences, such as the PRICAI'06, STMI'12, and BICS'16. He has served as a Program Committee Member for several international and native conferences, such as the IJCAI, AAAI, NIPS, SDM, PRICAI, and ACML. He is a member of the Machine Learning Society of the Chinese Association of Artificial Intelligence and the Artificial Intelligence and Pattern Recognition Society of the China Computer Federation.

Dinggang Shen (F'18) is the Jeffrey Houpt Distinguished Investigator and a Professor of radiology with the Biomedical Research Imaging Center (BRIC), computer science, and biomedical engineering with the University of North Carolina at Chapel Hill. He is currently directing the Center for Image Analysis and Informatics, the Image Display, Enhancement, and Analysis Laboratory, the Department of Radiology, and the medical image analysis core in the BRIC. He was a tenure-track Assistant Professor with the University of Pennsylvanian, and a Faculty Member with the Johns Hopkins University. He has published over 800 papers in the international journals and conference proceedings. His research interests include medical image analysis, computer vision, and pattern recognition. He serves as an editorial board member for eight international journals. He has also served in the Board of Directors, The Medical Image Computing and Computer Assisted Intervention Society, from 2012 to 2015. He is a fellow of the American Institute for Medical and Biological Engineering (AIMBE).